

CHARACTERIZATION AND MULTI-SCALE MODELING OF THE TRANSVERSE COMPRESSION OF THICK RTM-PROCESSED UNIDIRECTIONAL SAMPLES

J. Chevalier¹, Y.-A. Janssens¹, P.P. Camanho², T. Pardoen¹, F. Lani³

¹Institute of Mechanics, Materials and Civil Engineering (IMMC), Université catholique de Louvain, Place Sainte-Barbe, n2, L5.02.02, 1348 Louvain-la-Neuve, Belgium

Email: jeremy.chevalier@uclouvain.be

²2aDEMec, Faculdade de Engenharia, Universidade do Porto, Rue Dr. Roberto Frias, s/n, 4200-465, Porto, Portugal

³Any-Shape s.a., Rue de la digue, 37, 4400 Flémalle, Belgium

Keywords: Unidirectional composite, finite element analysis, RTM-processed composites, transverse compression

Abstract

Thick RTM-processed unidirectional (UD) samples were produced and tested under transverse compression. The experimental results were confronted to micro-mechanical analyses on representative volume elements (RVEs) with random fiber distributions and periodic boundary conditions. The matrix used is the RTM6 epoxy resin, whose curing cycle was used for the processing of the UD samples. Hence, a constitutive model developed for RTM6 could be used as an input parameter. A damage model for the matrix as well as cohesive elements with a traction-separation law for the fiber-matrix interfaces were also included. The comparison between the predictions and the experimental results and observations highlights the limitations related to the use of a constitutive model validated at the macro-scale, to model the matrix behaviour within the composite, involving a small length scale set by the fiber spacing.

1. Introduction

The proper modelling and the prediction of the mechanical behavior of fiber reinforced polymers (FRP) used in high-performance structural applications require accurate characterization of their constituents, that is, essentially, the interfaces (inter- and intra-laminar), the matrix and the fibers.

The (visco-)elasto-(visco-)plastic behavior of both thermoplastic and thermoset polymer matrices have been largely studied, leading to the development and the validation of various models addressing the rate, pressure and temperature dependence on the plastic yielding and on the failure of these polymeric materials [1–4]. Given the small-scale of the mechanisms associated to the interfaces between the fibers and matrix, the characterization of their mechanical response is very complicated. As a matter of fact, the first studies on the role played by the interfaces were dedicated to the observation of the influence of the interface resistance on the macroscopic response of the composite, mainly by varying the fiber surface treatment[5]. The direct determination of the actual properties of interfaces is a more recent subject of interest, mainly favored by the development of new characterization methods, such as the push-out/in of a single fiber in order to load a single interface [6–9]. However, despite recent progress, it is still a difficult task to clearly distinguish whether the failure is caused by matrix cracking very near the interface or by a true interfacial decohesion [9].

At the scale of a ply, many micro-mechanical analyses have been recently performed in order to analyze the influence of the input material parameters on the response of representative volume elements (RVEs) [10–18]. The goals of such analyses are numerous : to reveal the effect of the thermal residual stresses on the interfaces [10, 11], to quantify the effect of the ply thickness on the compressive strength [12], to determine the influence of the interfaces on the strength [13–15] or the influence of the loading mode on the failure locus [16]. However, there is still a lack of direct experimental validations demonstrating the accuracy of the predicted mechanical response with these simulated RVEs. Indeed, even though the failure loci seem to agree very well with the predictions made by the advanced fracture criteria for composite laminates [19, 20], the predicted strength and the stress at which damage is initiated inside the composite have rarely been confronted to experimental data.

Following these statements, the present work aims at studying whether the currently identified input ingredients are sufficient to accurately model the mechanical behavior of a unidirectional composite (UD) under transverse compression. The experimental results of cubic samples loaded in transverse compression at three different strain rates are used and compared to direct finite element (FE) analyses on 2D RVEs of the UD, under both plane strain and plane stress conditions. The manufacturing of the thick UD is itself a particularity of this work as it was made through a resin transfer moulding process (RTM) in order to perfectly replicate the curing conditions of the bulk matrix (RTM6 epoxy resin) which was used to identify the constitutive model parameters [3, 4].

2. Materials, processing and methods

2.1. Materials

The matrix is the monocomponent HexFlow RTM 6 epoxy resin, from Hexcel. The RTM 6 epoxy resin has been developed in order to be used in aeronautic and space industry applications, where it is usually utilized as a matrix in carbon fiber reinforced composites. It is supplied as a premixed system composed of tetra-glycidylmethylenedianiline (TGMDA) epoxy polymer and of two amine curing-agents M-DEA and M-DIPA. The RTM 6 resin has a high glass transition temperature $T_g = 220$ °C, extracted from differential scanning calorimetry (DSC), which guarantees good thermal stability and makes it suitable for use up to 180 °C.

2.2. Processing

The UD slab was manufactured by RTM. The carbon fibers were provided by Saertex GmbH as a +45° / –45° plain weave non crimp fabric. As a matter of fact, the fibers had to be unstitched in order to produce unidirectional fibers layers and a total of 34 layers was necessary in order to fill the 52x3x1 mm mould. Beforehand, the mould was coated with a release agent. The curing phase was exactly the same as the one used for the bulk matrix. First, a heating ramp from 90°C to 130°C at a heating rate of 2°C/min was applied. It was followed by a low-temperature curing cycle at 130°C during 3h. Then, a three hour post-curing step was imposed at 180°C, with a heating ramp of 2°C/min. The UD slab was cooled down at a cooling rate of 10°C/min. An analysis of micrographs obtained with an optical microscope at randomly chosen spots in the slab enabled the calculation of an average fiber volume fraction of around 40%.

2.3. Testing methods

Cubic samples of 10mm long edges were machined from the UD slab. The transverse compression tests were performed on a screw-driven universal testing machine (Zwick-Roell with an external loading cell of 250 kN). The axial displacement was measured using a compliance corrected crosshead displacement

method. All tests were performed at room temperature and three different true strain rates were used : $\dot{\epsilon} = 10^{-4}$, 10^{-3} and 10^{-2}s^{-1} . Three samples were tested for each strain rate. The friction could be minimized thanks to PTFE films inserted between the platens of the testing machine and the specimens.

2.4. Finite element modelling

Finite element analyses were carried out using the commercial code Abaqus [Ref manual]. Several 2D square RVEs of dimension $L \times L$ were created using a simple script randomly positioning fibers inside the matrix. As the fiber volume fraction measured in the samples was below 0.50, it was not necessary to use algorithms such as the one developed by Melro et al. [21]. Four different RVEs with $L = 50\mu\text{m}$ were generated in order to assess the variability related to the different configurations and one RVE with $L = 100\mu\text{m}$ was generated in order to determine the effect of the RVE size. The fibers were supposed to all have the same radius $R_f = 5\mu\text{m}$. Both plane strain and plane stress conditions are examined. Periodic boundary conditions (PBC) were applied to the edges of the RVEs. While it has already been stated that PBC affect the damage pattern once failure is initiated in the RVE [14], it was not the focus of the present work to characterize this pattern.

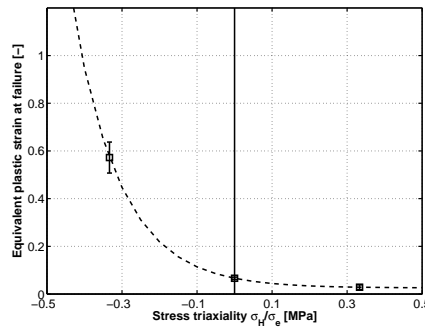


Figure 1: Critical equivalent strain at failure criterion identified with compression, tension and torsion experimental data on the RTM6 epoxy resin [4]

The fibers were supposed to remain linear elastic throughout the simulation, with a Young's modulus $E_f = 19.5\text{GPa}$ and a Poisson ratio $\nu_f = 0.28$. The matrix was modelled as elastic plastic with a rate-dependent hardening law. The pressure dependence on the yield surface of the matrix was described by a linear Drucker-Prager model, which write in the $(\sigma_e, \frac{\sigma_{kk}}{3})$ plane

$$F = \sigma_e + \frac{\sigma_{kk}}{3} \tan \beta - \left(1 - \frac{\tan \beta}{3}\right) \sigma_c = 0 \quad (1)$$

with σ_e being the Von Mises equivalent stress, σ_{kk} the trace of the Cauchy stress tensor, β the friction angle and σ_c the yield stress in pure compression. The model was validated under six decades of strain rates with $\beta = 7.86$ and the dilation angle equal to 0. A fracture criterion is also added in the description of the matrix model. It is a stress triaxiality-dependent critical equivalent plastic strain criterion, which has been identified using uniaxial tensile, pure compression and torsion tests on bulk resin samples. Fig. 1 shows the description of the criterion in the equivalent plastic strain/stress triaxiality plane. It is implemented as a ductile damage criterion in Abaqus with a fracture energy set at $1\text{J}/\text{mm}^2$. The elastic properties of the matrix are given by $E_m = 3\text{GPa}$ and $\nu_m = 0.34$. The modelling of the mechanical behavior of the RTM6 epoxy resin, which was the matrix considered in this work, is extensively described

in the work of Lani [3] and Morelle [4]. The interfaces between the fibers and the matrix were modelled using cohesive elements whose mechanical behavior was described by a linear traction-separation law. The properties of the interfaces are taken from Arteiro et al.[12] and are shown in Table 1. Abaqus Explicit is used to overcome convergence issues caused both by the softening in the strain-stress curve of the matrix and by the progressive damage and eventual failure of the matrix and the cohesive elements. Therefore, as generalized plane strain elements are not available in Abaqus Explicit, both plane strain and plane stress conditions were tested. Even though the authors realize that such conditions overly simplify the real stress and strain states in the RVEs, it is believed that it gives a sufficiently thin interval in which the real solution lies, which is sufficient to address the ability or not of the identified constituents' behavior to properly model the response of the UD cubic specimens. The interfaces are modelled using 4-node two-dimensional cohesive elements (COH2D4) [22]. Both the matrix and the fibers are modelled using 3-node linear elements (CPE3 and CPS3 respectively for plane strain and plane stress conditions) [22]. The element size was set to be approximately $0.1 \times R_f$, giving an approximate total number of elements equal to 28 000 for the small RVEs and 110 500 for the large RVE.

Table 1: Mechanical properties of the interfaces

Material property	K (GPa)	τ_1^0 (MPa)	τ_2^0 (MPa)	τ_3^0 (MPa)	G_{Ic} (N/mm)	G_{IIc} (N/mm)	G_{IIIc} (N/mm)	η (BK law) (-)
Value	10^8	75	75	50	0.002	0.006	0.006	1.45

3. Experimental results

Fig. 2 shows the true stress true strain curves obtained from the transverse compression tests on the UD cubic samples at three different strain rates. Fig. 3a and Fig. 3b respectively illustrate the influence of the strain rate on the Young's modulus and on the fracture stress and fracture strain of the UD. As expected, the stiffness varied around 4000MPa and is not influenced by an increase in strain rate. Reversely, and even though only two decades of strain rates have been tested, the influence of the strain rate is noticeable with a slight increase of the fracture stress and of the fracture strain with an increase of the strain rate. This effect is not a surprise, given the visco-plastic behavior of the matrix [4]. This effect is more marked when working at much higher rates, as displayed, for example by Koerber et al. [23].

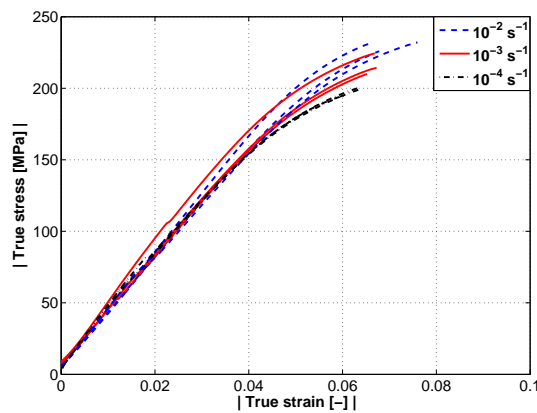


Figure 2: True stress true strain curves from the transverse compression tests at three different true strain rates.

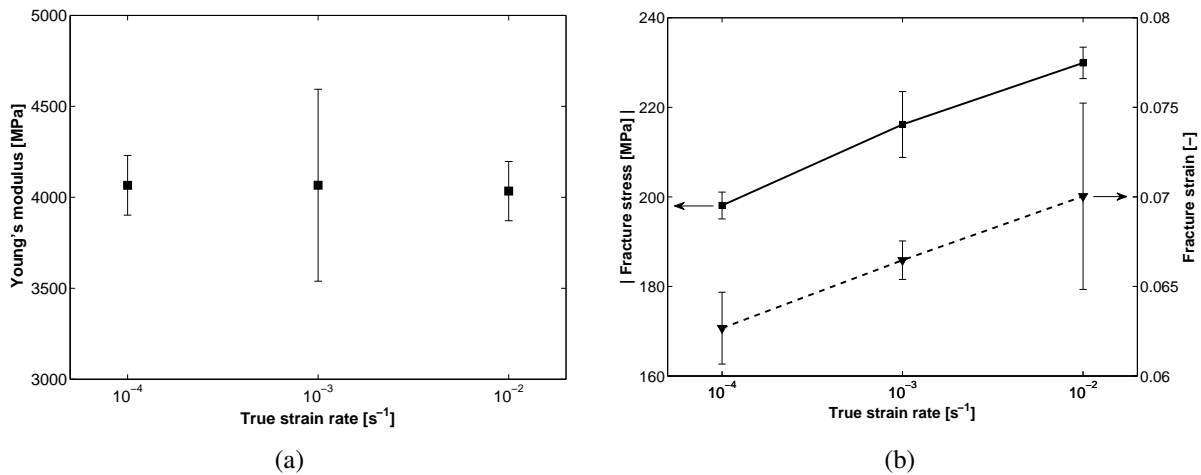


Figure 3: a) Young's modulus of the UD specimens in the transverse direction for each strain rate; b) evolution of the true fracture stress and strain with respect to the true strain rate.

4. FEA results and discussion

The finite element analyses consisted in a transverse compression load applied to four different small RVEs and one large RVE, all of them with a volume fraction of fibers $V_f = 0.40$. The stress-strain curves were obtained by volumetric homogenization. Most of the results will be displayed for all cases, as for stress-strain curves, or shown as an average over the different RVEs tested, as for the fracture stress and strain. However, when a single result is shown, as for a contour plot of a given variable for example, it is representative of what was observed in all of the other cases.

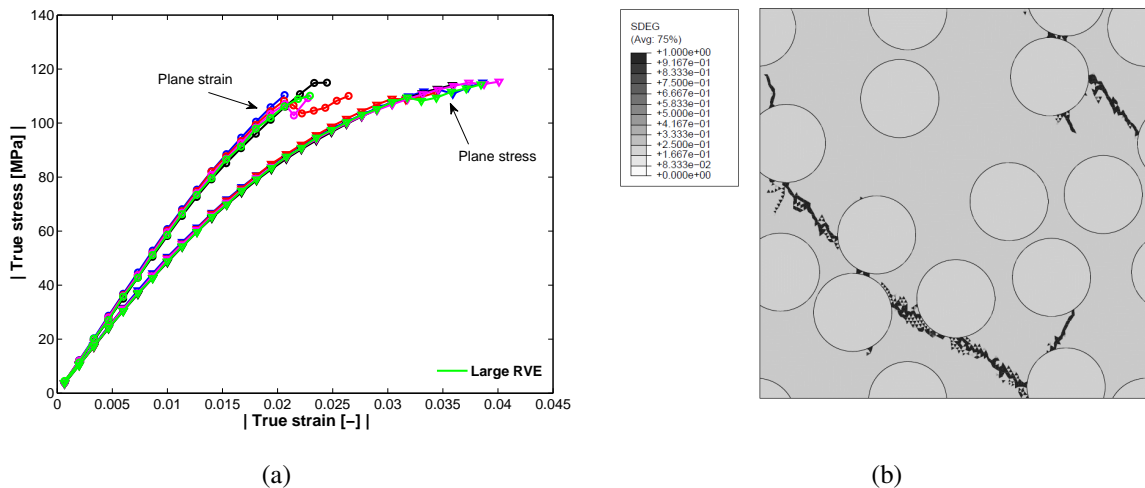


Figure 4: a) True stress - true strain curves from the transverse compression tests at three different true strain rates; b) contour plot showing the damage pattern on one of the small RVEs after failure.

Fig. 4a shows the true strain - true stress curves obtained for each RVEs tested under transverse compression at $\dot{\epsilon} = 10^{-4}$. As explained in section 2.4, the curves are shown for both plane stress and plane strain conditions. The curves are stopped at the maximum stress reached during the simulations, corresponding to the onset of generalized damage both in the matrix and in the cohesive elements. However, it is possible that a small number of elements had already failed when the stress reaches its maximum, as highlighted by the small drops observed in some of the curves. As expected, the RVEs under plane strain

Excerpt from ISBN 978-3-00-053387-7

conditions display a stiffer response and less non-linearity. Moreover, the stress-strain curve of the large RVE does not highlight any shortcoming linked to the use of small RVEs. Fig. 4b shows the damage patterns in a failed small RVE at the end of the simulation. The orientation of this band of damage is around 50° with respect to the applied load direction, which is clearly in line both with experimental observations and simulations results [13, 14, 16].

The shape of the curves and the fracture stress is clearly in line with calculations made in previous micro-mechanical analyses considering the case of transverse compression applied to UD RVEs. Indeed, even though the mechanical properties of the constituents vary depending on the model chosen for the interfaces and the matrix, previous works mostly treat the case of a thermoset matrix and cohesive elements to model the interfaces between the fibers and the matrix. Therefore, there is no surprise in predicting a fracture stress between 100 and 150 (or slightly over 150)MPa in most of the micro-mechanical analyses performed [10, 13–17]. However, the comparison between the predictions of Fig. 4a and the experimental curves of Fig. 2 indicate that the fracture strain and fracture stress are clearly underestimated.

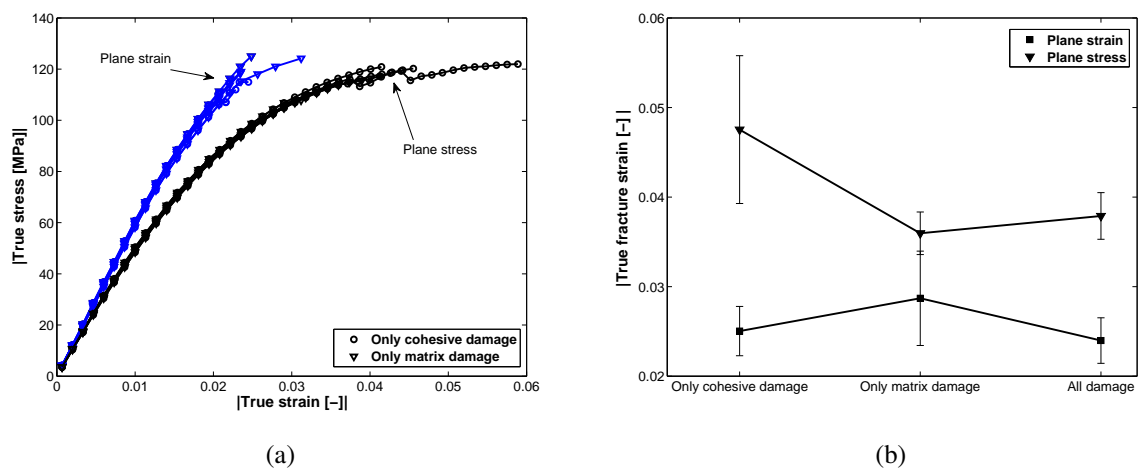


Figure 5: a) True stress true strain curves obtained from the simulations on the RVE, simulations with damage only in the matrix and damage only in the cohesive elements are illustrated; b) dependence of the true fracture strain attained in the simulations depending on the damage models which are incorporated in the model of the RVE.

An early failure of the RVEs could be directly related to the difference between the scale of the RVEs and the scale at which the fracture criterion of the matrix has been identified. Indeed, the failure of brittle materials, such as epoxy resins, can generally be explained by the presence of critical defects inside the materials which lead to the attainment of much larger stresses locally than the ones applied to the bulk material [24]. As a matter of fact, failure criteria identified at the macro-scale, on bulk specimens, assume the existence of a population of defects such that there is always very sharp defects in the zone subjected to the critical stress state at the macro-scale. When working at the micro-scale, like in such analyses on RVEs, the element size has a physical meaning. Indeed, if the criterion identified at the macro-scale is used in the RVE, each element is assumed to contain the exact same population of defects as the bulk specimens. As a matter of fact, this kind of fracture criterion should be used very cautiously at the micro-scale. In order to illustrate the impact of the failure criterion of the matrix on the response of the RVE, Fig. 5a shows the stress-strain curves obtained without any damage in the matrix but damage in the cohesive elements and the opposite. As illustrated, there is no any difference between both cases, meaning that both the matrix and the cohesive elements fail almost simultaneously during the simulation. Hence, the selected failure criteria seem to be a reason for the gap between the experimental and the simulation results. Fig. 6a superposes the experimental stress-strain curves at $\dot{\epsilon} = 10^{-4}\text{s}^{-1}$ with

the homogenized ones obtained by FEA for a representative configuration. Clearly, the description of the matrix plastic yielding appears to be inaccurate, despite a very good agreement at the macro-scale [4] as the non-linearity observed in the simulations is much more pronounced than the experimental response.

The inaccuracy of the matrix plastic yielding description could be directly related to the validation process of the constitutive model of the resin at the macro-scale. Indeed, as often, the range of stress triaxialities which has been used in order to validate the model was bounded by the pure compression and uniaxial tension tests, i.e. between $-1/3$ and $1/3$. Fig. 6b shows a histogram of the stress triaxialities among all the matrix elements of the large RVE mesh at an applied stress of 45MPa, in both plane stress and plane strain conditions. Clearly, a significant part of the elements are outside of the boundaries fixed by the validation process. As a matter of fact, the effect of the pressure on the mechanical response of these elements could be wrongly described by the linear Drucker-Prager model.

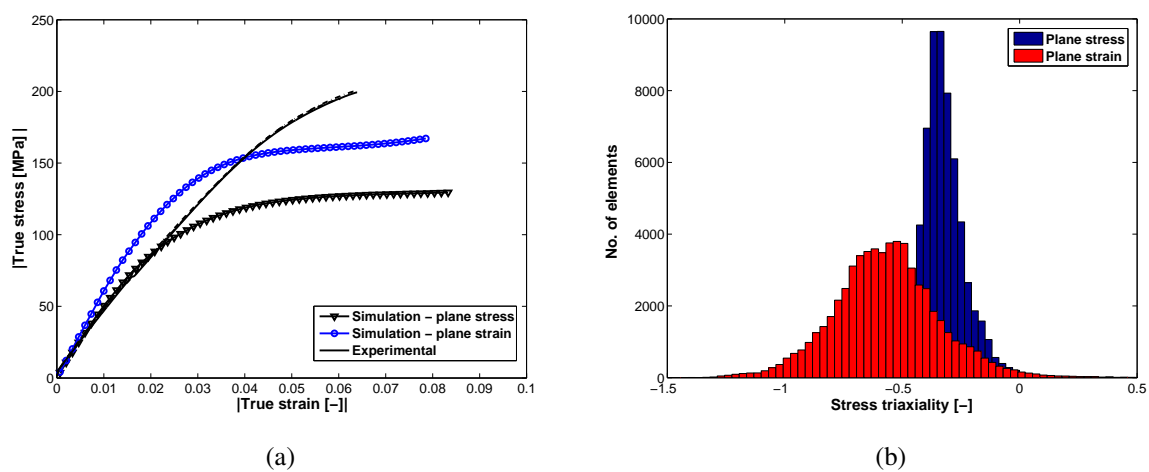


Figure 6: a) Superposition of the true strain - true stress experimental curves at $\dot{\epsilon} = 10^{-4} \text{s}^{-1}$ and of the homogenized curve of simulations in plane stress and plane strain of a representative RVE, when no damage in the matrix and in the cohesive elements is included; b) histogram of the stress triaxialities among all the matrix elements in the large RVE with an applied stress of 45MPa, at $\dot{\epsilon} = 10^{-4} \text{s}^{-1}$, both in plane strain and plane stress conditions.

However, even though the properties of the interfaces seem to be too low because of the early failure of the RVE that they induce, they may not be the sole responsible for this effect. Indeed, it is observed that the load capability of the RVEs is drastically altered by the failure of the first interface. It seems that once an interface has failed, the load cannot be properly transferred to the pristine regions in the RVE. However, the observations on the progressive damage in fiber reinforced polymers rather show that a progressive damage takes place before the actual failure of the material. Hence, the composite does not fail as soon as a fiber-matrix interface fails. As a matter of fact, the size of the RVE may have to be reconsidered. Fig. 4a shows that a four times larger RVE does not display a different true stress - true strain curve than the one obtained on the small RVEs. Yet, when considering the damage caused by the interface, the load transfer capability from the damaged zones to the undamaged ones should be drastically improved by an increase of the RVE size.

As shown by Morelle [4], the plastic yielding of RTM6 strongly depends on the strain rate. Fig. 3b illustrates a similar effect on the response of the UD cubic samples, which is caused by its matrix. Therefore, as the model for the matrix included in the simulations accounts for that strain rate dependency, it should also be translated to the homogenized response of the RVEs. Fig. 7 shows the effect of the strain rate

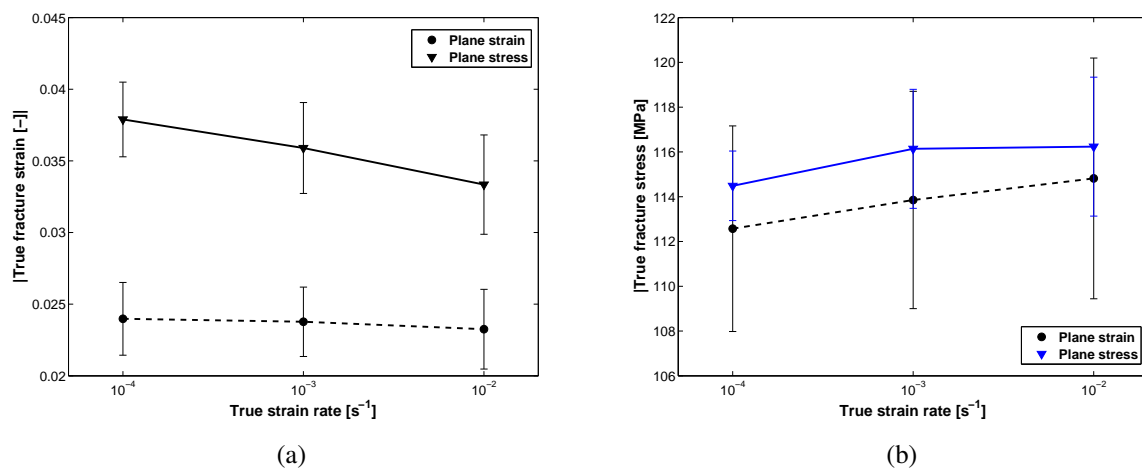


Figure 7: a) Reference load-displacement curves of the tensile tests on notched specimens; b) variation of the maximum principal stress as a function of the distance to the notch root right at failure, computed by FE analyses.

on the fracture strain and fracture stress calculated by the simulations. The fracture stress increases with the strain rate, as expected, albeit much more slightly than on the cubic samples. The small amplitude of the strain rate influence is believed to be mainly caused by the earlier fracture obtained in the simulations, and that the difference between the fracture stresses at the three strain rates is likely to increase if the fracture was to happen later during the loading of the RVE. Conversely and unlike the experimental observations, the fracture strain decreases as the strain rate increases. Indeed, a higher strain rate leads to a stiffer response of the matrix, meaning that the applied deformation is not accommodated as well by the matrix. Hence, the solicitation on the interfaces is larger and the failure of the first interface occurs earlier at a higher strain rate.

5. Conclusion

The proper modelling of FRP is believed to necessitate as input arguments models that accurately predict the mechanical behaviour of their constituents. Hence, simulations of RVEs of a UD composite under transverse compression have been performed and compared to experimental results obtained on cubic samples. The samples were machined from a slab which was produced by RTM, enabling the exact same curing cycle as the one used for the characterization of the bulk matrix. Therefore, the model for the matrix behaviour incorporated in the simulations was believed to accurately capture its pressure- and rate-dependence on the yielding and the failure initiation. The comparison of the micro-mechanical study on the RVEs with the experimental observations led to the following developments and conclusions :

- A thick slab of RTM-processed unidirectionnal composite could be produced, enabling the use of the constitutive model developed for the RTM6 epoxy resin by Morelle [4].
- As illustrated by the proper orientation of the damaged zone in the matrix, which can be directly related to the accumulation of plastic strain, the linear Drucker-Prager model captures the plastic strain localization process within the matrix well.
- The numerical predictions of the fracture strain and of the fracture stress clearly underestimate the experimental values, showing the inadequacy of using a fracture criterion identified at the macro-scale for the matrix.

- The size of the RVE becomes significant when damage at the interfaces is considered, as increasing the size of the RVE will increase the load transfer capability of the RVE to the undamaged zones.
- The linear Drucker-Prager predicts a non-linear behavior of the homogenized composite largely superior than the one experimentally observed, because of the massive yielding and softening in the matrix.

Overall, this study mainly highlights the issues related to the use of a matrix constitutive model which has been identified on bulk resin specimens at the macro-scale to model its mechanical behaviour within a UD composite. Practically, it has been shown that the effect of the pressure on the mechanical response of the resin within the composite had not been validated through the linear Drucker-Prager model, as a significant part of the elements in the mesh are submitted to stress triaxialities out of the range under which the model was validated. Physically, it is still unclear if the presence of the fibers could have an influence on the curing of the resin or have a constraining effect on the mechanisms responsible for the plastic yielding of the resin. Moreover, the use of a fracture criterion validated on pure resin at the macro-scale implies that each element contains the exact same statistical distribution of defects as the macro specimens. Hence, such criteria are not well suited to predict the matrix failure within a composite.

Acknowledgments

The authors acknowledge the financial support of the Interuniversity Attraction Poles Program from the Belgian State through the Belgian Policy agency, contract IAP7/21 INTEMATE. J. Chevalier acknowledges the financial support of the FRIA, Belgium. Computational resources have been provided by the supercomputing facilities of the Université catholique de Louvain (CISM/UCL) and the Consortium des Equipements de Calcul Intensif en Fédération Wallonie Bruxelles (CECI) funded by the Fonds de la Recherche Scientifique de Belgique (FRS-FNRS).

References

- [1] R. Gerlach, C.R. Siviour, N. Petrinic, and J. Wiegand. Experimental characterisation and constitutive modelling of rtm-6 resin under impact loading. *Polymer*, 49(11):2728–2737, 2008.
- [2] X. Poulain, A.A. Benzerga, and R.K. Goldberg. Finite-strain elasto-viscoplastic behavior of an epoxy resin: Experiments and modeling in the glassy regime. *International Journal of Plasticity*, 62:138–161, 2014.
- [3] F. Lani, X.P. Morelle, C. Bailly, and T. Pardoën. Characterization and modeling of the strain-rate, temperature and pressure dependence of the deformation of a highly cross-linked aerospace grade epoxy resin. *ICCM 2015 - Composites at Copenhagen, Proceedings of the 20th International Conference on Composite Materials*, 2015.
- [4] Xavier Morelle. *Mechanical characterization and physics-based modeling of a highly-crosslinked epoxy resin*. PhD thesis, Université catholique de Louvain, 2015.
- [5] S. Subramanian, J.J. Lesko, K.L. Reifsnider, and W.W. Stinchcomb. Characterization of the fiber-matrix interphase and its influence on mechanical properties of unidirectional composites. *Journal of Composite Materials*, 30(3):309–332, 1996.
- [6] H. Zhang, M.L. Ericson, J. Varna, and L.A. Berglund. Transverse single-fibre test for interfacial debonding in composites: 1. experimental observations. *Composites Part A: Applied Science and Manufacturing*, 28(4):309–315, 1997.

- [7] J. Varna, L.A. Berglund, and M.L. Ericson. Transverse single-fibre test for interfacial debonding in composites: 2. modelling. *Composites Part A: Applied Science and Manufacturing*, 28(4):317–326, 1997.
- [8] M. Rodríguez, J.M. Molina-Aldaregua, C. Gonzalez, and J. Llorca. A methodology to measure the interface shear strength by means of the fiber push-in test. *Composites Science and Technology*, 72(15):1924–1932, 2012.
- [9] J. Jäger, M.G.R. Sause, F. Burkert, J. Moosburger-Will, M. Greisel, and S. Horn. Influence of plastic deformation on single-fiber push-out tests of carbon fiber reinforced epoxy resin. *Composites Part A: Applied Science and Manufacturing*, 71:157–167, 2015.
- [10] T.J. Vaughan and C.T. McCarthy. A micromechanical study on the effect of intra-ply properties on transverse shear fracture in fibre reinforced composites. *Composites Part A: Applied Science and Manufacturing*, 42(9):1217–1228, 2011.
- [11] T.J. Vaughan and C.T. McCarthy. Micromechanical modelling of the transverse damage behaviour in fibre reinforced composites. *Composites Science and Technology*, 71(3):388–396, 2011.
- [12] A. Arteiro, G. Catalanotti, A.R. Melro, P. Linde, and P.P. Camanho. Micro-mechanical analysis of the effect of ply thickness on the transverse compressive strength of polymer composites. *Composites Part A: Applied Science and Manufacturing*, 79:127–137, 2015.
- [13] L. Yang, Y. Yan, Y. Liu, and Z. Ran. Microscopic failure mechanisms of fiber-reinforced polymer composites under transverse tension and compression. *Composites Science and Technology*, 72(15):1818–1825, 2012.
- [14] A.R. Melro, P.P. Camanho, F.M. Andrade Pires, and S.T. Pinho. Micromechanical analysis of polymer composites reinforced by unidirectional fibres: Part {II} micromechanical analyses. *International Journal of Solids and Structures*, 50(1112):1906 – 1915, 2013.
- [15] Y. Hu, N.K. Kar, and S.R. Nutt. Transverse compression failure of unidirectional composites. *Polymer Composites*, 36(4):756–766, 2015.
- [16] E. Totry, C. Gonzalez, and J. LLorca. Failure locus of fiber-reinforced composites under transverse compression and out-of-plane shear. *Composites Science and Technology*, 68(3-4):829–839, 2008.
- [17] C. Gonzalez and J. LLorca. Mechanical behavior of unidirectional fiber-reinforced polymers under transverse compression: Microscopic mechanisms and modeling. *Composites Science and Technology*, 67(13):2795–2806, 2007. cited By 113.
- [18] L.P. Canal, C. Gonzalez, J. Segurado, and J. LLorca. Intraply fracture of fiber-reinforced composites: Microscopic mechanisms and modeling. *Composites Science and Technology*, 72(11):1223–1232, 2012.
- [19] A. Puck and H. Schurmann. Failure analysis of {FRP} laminates by means of physically based phenomenological models. *Composites Science and Technology*, 62(1213):1633 – 1662, 2002.
- [20] S.T. Pinho, R. Darvizeh, P. Robinson, C. Schuecker, and P.P. Camanho. Material and structural response of polymer-matrix fibre-reinforced composites. *Journal of Composite Materials*, 46(19-20):2313–2341, 2012.
- [21] A.R. Melro, P.P. Camanho, and S.T. Pinho. Generation of random distribution of fibres in long-fibre reinforced composites. *Composites Science and Technology*, 68(9):2092–2102, 2008.
- [22] ABAQUS 6.12/Standard Users Manual. Hibbit, Karlsson and Sorensen Inc., Pawtucket, RI, 2012.

- [23] H. Koerber, J. Xavier, and P.P. Camanho. High strain rate characterisation of unidirectional carbon-epoxy im7-8552 in transverse compression and in-plane shear using digital image correlation. *Mechanics of Materials*, 42(11):1004–1019, 2010.
- [24] J. Chevalier, X.P. Morelle, C. Bailly, P.P. Camanho, T. Pardoën, and F. Lani. Micro-mechanics based pressure dependent failure model for highly cross-linked epoxy resins. *Engineering Fracture Mechanics*, 158:1–12, 2016.